Enhancement of silicon solar cells by downshifting with Eu and Tb coordination complexes

T. Fix, A. Nonat, D. Imbert, S Di Pietro, M. Mazzanti, A. Slaoui, L. J Charbonnière

Enhancement of silicon solar cells by downshifting with Eu and Tb coordination complexes

T. Fix[1*], A. Nonat[2*], D. Imbert[3], S. Di Pietro[3], M. Mazzanti[4], A. Slaoui[1] and L. J. Charbonnière[2]

[1] ICube laboratory (Université de Strasbourg and CNRS), 23 rue du Loess BP 20 CR, 67037 Strasbourg Cedex 2, France. E-mail : thomas.fix@unistra.fr

[2] Laboratoire d'Ingénierie Moléculaire Appliquée à l'Analyse, IPHC, UMR 7178 CNRS, Université de Strasbourg, ECPM, Bât R1N0, 25 rue Becquerel, 67087 Strasbourg Cedex, France. E-mail : aline.nonat@unistra.fr

[3] Univ. Grenoble Alpes, INAC-SCIB, F-38000 Grenoble, France; CEA, INAC-SCIB, F-38000 Grenoble, France.

[4] Institut des Sciences et Ingénierie Chimiques, Ecole Polytechnique Fédérale de Lausanne (EPFL), 1015 Lausanne (Switzerland)

Abstract.

Luminescent lanthanide-doped oxides, nanoparticles, nanocrystals and coordination complexes are major tools in the fields of optical and LASER materials, telecommunications, medical imaging and fluoroimmunoassays. In particular, coordination complexes are efficient energy converters with high photostability, large ligand-induced Stokes shifts and tunable excitation and emission spectra. However, their application as light downshifting materials for solar cells has not yet been widely explored. This third generation solar cell concept enables to increase the efficiency of standard solar cells − such as Si or CIGS − that have low performance for ultraviolet photons. The incorporation of such a converter in solar module encapsulants can provide a cheap and effective way to integrate photon conversion. Here, encapsulants functionalised by photon downshifting coordination complexes have been spin-coated on silicon solar cells. For all the coordination complexes, an increase of the spectral response of the solar cells is observed in the ultraviolet region. In the best case, a relative increase of 8% of the conversion efficiency of the solar cell is observed.

Keywords: downshifting, photon conversion, photoluminescence, polymer, Lanthanide complex

1. Introduction

Downshifting, downconversion (quantum cutting) and upconversion are third-generation advanced concepts for solar cells[1]. They aim to reduce the losses in single bandgap photovoltaic systems, either due to the thermalisation of photons having an energy higher than the band gap (*ie.* in the 280 – 400 nm spectral range) or due to the non absorption of photons having an energy lower than the band gap. These two mechanisms lead to about 50% of the losses in the conversion into electricity in single bandgap systems. To reduce these losses, three photon conversion concepts have been proposed: downshifting (where an ultraviolet (UV) photon is converted into a visible or infrared (IR) photon)[2], downconversion (a UV photon is converted into two visible or IR photons)[3,4], or upconversion (two IR photons are converted into a visible photon)[5-7]. Huang and coworkers have recently published an interesting review of spectral converters.[8]

To date, downconversion has not led to significant improvements and better systems need to be developed.[9-11] This is due principally to the low quantum yield of these systems, generally based on rare earth element doped oxides. In this field, the observation of the spectral response of the solar cells is the key to determine if the improvement of the solar cells is due to photon conversion rather than a simple passivation or antireflective effect. However, there have been several studies showing improvements of solar cells using various luminescent downshifting (LDS) materials such as organic dyes,[12,13] quantum dots (QDs),[12] or rare earth coordination complexes – mainly Eu(III) complexes,[12-20] which is the scope of the present article. Indeed, Eu(III) coordination complexes have many advantages since they are highly luminescent and photostable. For instance, the complex $[Eu(tta)_3(tppo)_2]$ (Figure 1) has been found to be stable for hours upon irradiation at 350 nm (13 h, when incorporated into a polystyrene matrix),[21] whereas common organic dyes decompose in few minutes, porphyrin derivatives and QDs in few hours.[22-24] $[Eu(tta)_3(tppo)_2]$ is also unaffected by thermal decomposition under 250°C.[21] Moreover, Eu(III) complexes are characterized by broad and tunable absorption bands in the 280 – 400 nm region with an emission profile centered at 615 nm, in perfect match with the maximum quantum efficiency of crystalline silicon (c-Si) based solar cells and which correspond to the $^5D_0 \rightarrow {}^7F_2$ electronic transition of Eu(III)[25]. They display significantly larger Stokes shifts than fluorescent dyes or QDs, which totally suppress losses due to self-absorption. Tb(III) complexes can also be used and, although the examples of complexes with quantitative quantum yields remain scarce, few examples have been reported in the literature with values above 95% in solution[26-28] and in the solid state.[26]

However, this can be partially offset by a less appropriate emission profile of the $^5D_4 \rightarrow {}^7F_J$ (J = 6-3), with a maximum at 545 nm. Indeed, luminescence of 4f coordination complexes is achieved by indirect excitation via a bound chromophoric unit: "the antenna". This sensitization mechanism –also called "antenna effect" – generally involves three steps: (i) excitation of the antenna to its singlet excited state, (ii) inter-system crossing (ISC) to the antenna's triplet state, and (iii) intramolecular energy transfer (ET) from the antenna to the accepting levels of the lanthanide ($^5D_0$ at 17200 $cm^{-1}$for Eu(III)and $^5D_4$ at 20400 cm^{-1} for Tb(III)). This mechanism results in long-lived emission in the ms range from the lanthanide and large ligand-induced Stokes shifts. As a consequence, the energy transfer efficiency can be optimized by an appropriate choice of the antennae and in particular by a good positioning of the energy level of their triplet states with respect to the excited state of the 4f ion of interest[29,30]. The absolute quantum yield of a complex is the combination of the energy transfer efficiency and of the intrinsic quantum yield of the metal ion in the complex, the latter being metal dependent and strongly influenced by the coordination geometry of the complex by its environment[31].

A possible and attractive way to use these materials is to incorporate them in the encapsulant of photovoltaic modules. In industry, ethylene-vinyl-acetate (EVA) matrixes are usually used and they are doped with UV absorbers in order to prevent their photochemical degradation (also called "yellowing")[32]. Using LDS materials instead of these additives provides the advantage that the UV photons are not lost but converted in visible photons, that provide a short-circuit current enhancement in the solar cells. These LDS encapsulants can also be used for organic and dye-sensitized solar cells in order to prevent the degradation of the solar cells due to the UV photons. As an illustration of the state of the art in this field, previous studies using Eu(III) complexes in LDS materials have been summarized in Table 1 and the corresponding chemical formulae are depicted in Figure 1. From these results it appears that ternary complexes with β-diketonate ligands such as [$Eu(tta)_3$phen], [$Eu(tta)_3$bpbpy] and [$Eu(hfa)_3(tppo)_2$] are strong candidates to be used in LDS materials. However, for a same dopant ([$Eu(tta)_3$phen], for instance), results have been shown to be strongly dependent of the composition of the LDS material (encapsulant, concentration…).

Losses in energy in LDS systems on solar cells mainly occur from non unity quantum yield of the LDS material, reflectivity of the LDS+solar cell system, but also from the downshifting principle itself (i.e. a 350 nm photon converted into a 610 nm photon represents an intrinsic loss in energy of about 40%).

In this work, doped EVA films have been prepared on top of crystalline Si solar cells. A series of four Ln(III) complexes, namely [Eu(tta)$_3$phen], [Eu(tta)$_3$(tppo)$_2$], [EuL$_3$] and [TbL$_3$] (Figure 1) have been compared and studied in similar conditions. We show that a significant improvement in solar cells can be obtained thanks to the LDS encapsulant.

2. Experimental

Synthesis of the complexes

Solvents and starting materials were purchased from Sigma-Aldrich, Acros and Alfa Aesar and used without further purification. [Eu(tta)$_3$phen] was synthesized in one step from 2-thenoyltrifluoroacetone, 1,10-phenanthroline and the europium(III) chloride salt according to the procedure previously described by Kadjane *et al*[37] and was obtained in 91% yield. Elemental composition (in weight %) has been confirmed by C, H, N elemental analysis at the Service Commun d'Analyse de l'Université de Strasbourg. $C_{36}H_{20}N_2O_6S_3Eu.2H_2O$: calcd. C 41.91, H 2.34, N 2.71; found C 41.71, H 2.03, N 2.71. The [Eu(tta)$_3$(tppo)$_2$] complex was obtained in two steps from [Eu(tta)$_3$(H$_2$O)$_2$] by following the procedure recently published by Lima *et al*[35] with an overall yield of 40%. $C_{60}H_{42}F_9O_8P_2S_3$: calcd. C 52.52, H 3.09, N 0.00; found C 52.47, H 3.16, N 0.00. The complexes [LnL$_3$](Et$_3$NH)$_3$ (Ln = Eu, Tb) containing the triazole-pyridine-bis-tetrazolate antenna, were isolated as their triethylamonium salts in 62% and 95 % yields, respectively, according to the procedure recently described by S. Di Pietro *et al*[26]. Complexes were characterized by mass spectrometry. For [Eu(tta)$_3$phen] and [Eu(tta)$_3$(tppo)$_2$], characteristic photophysical properties such as their luminescent lifetime and quantum yield, were compared with previously published values.

Preparation of the polymeric luminescent films

Six chloroform solutions of the coordination complexes at various concentrations were prepared and dissolved in an ultrasonic bath. The composition (complex /mass of complex in g/mass of CHCl$_3$ in g) of the samples is as follows: [Eu(tta)$_3$phen]/0.0054/14.5; [Eu(tta)$_3$phen]/0.0108/14.5; [Eu(tta)$_3$(tppo)$_2$]/0.0267/14; [Eu(tta)$_3$(tppo)$_2$]/0.0537/14; [EuL$_3$]/0.0160/14.5; [TbL$_3$]/0.0161/14.5. Then ethylene vinyl acetate pellets (Sigma-Aldrich 33 wt.%) (2 g) were dissolved in the solutions. In further studies, the concentration of the complexes is indicated in weight % relative to the mass of EVA in solution. The mixture is then spin coated on quartz substrates or on PN junction silicon solar cell structures. The films are cured for one hour at 80°C, films are in the order of 5 µm thickness as measured with an Eddy currents tool (Elcometer).

Spectroscopic characterization of the complexes and of the luminescent films

Transmittance spectra were obtained with a UV VIS NIR Lambda 19 Perkin Elmer spectrophotometer using a normal incidence. Steady state emission and excitation spectra (defined as photoluminescence, PL, and photoluminescence excitation, PLE, in the text) were recorded on a Horiba Jobin Yvon Fluorolog 3 spectrometer working with a continuous 450W Xe lamp. For the measurements in the solid state and for the characterization of the films on quartz plates or on solar cells, the spectrometer was fitted with an integrating sphere Quanta-Φ from Horiba. Detection was performed with a Hamamatsu R928 photomultiplier. All spectra were corrected for the instrumental functions. When necessary, a 399 nm cut-off filter was used to eliminate second order artefacts. Phosphorescence lifetimes were measured on the same instrument working in phosphorescence mode and with a Xenon flash lamp as the excitation source. Mono-exponential and multi-exponential emission decay profiles were fitted with the Datastation software from Jobin Yvon. Luminescence quantum yields of diluted solutions (o. d. < 0.05) were measured according to conventional procedures, using $[Ru(bpy)_3]Cl_2$ in non-degassed water (Φ = 4.0%) as reference.[38] The estimated errors are ± 15%.

Double determination of the absolute luminescence quantum yields of the luminescent films was performed according to the procedure described in reference[26] by using a Hamamatsu Quantaurus-QY integrating sphere and an integrating sphere from GMPS.A. (Switzerland) coupled to the Fluorolog 3 spectrofluorimeter.

Reflectance measurements were performed in the 300-800 nm range in the Quanta-Φ integration sphere (see Supplementary Material for further details).

Characterization of the solar cells

For the tests on solar cells, n^+p silicon solar cells were used. The n^+ emitter was prepared by thermal diffusion of phosphorus from a spin-on dopant glass layer into a 1 Ω·cm p-type doped silicon Cz <001> wafer. A SiN antireflective coating was deposited by plasma-enhanced chemical vapor deposition. The front grid contact was made of Ti/Pd/Ag using the photolithography technique, while the back contact is a plane evaporated aluminum layer.

For solar cell characterization, the setup used for our external quantum efficiency (EQE) measurements consists of a light source (tungsten halogen) and automated filter wheels with appropriate order sorting filters; 41 filters are used for the measurements with a Keithley 2400 SourceMeter. The EQE measurement involves the ratio of current produced on the sample

solar cell at a given wavelength to the current generated by a certified reference detector at the same wavelength. The EQE measurement accuracy was checked with a secondary certified reference. I-V characteristics were performed using an Oriel Solar Simulator in AM1.5G conditions. The solar cells provide an efficiency before coating of around 9 %, which is due to a low fill factor (independent from the present study).

3. Results and discussion

In this study, four strongly emitting Ln(III) complexes, namely [Eu(phen)$(tta)_3$], [Eu$(tta)_3(tppo)_2$], [EuL_3] and [TbL_3] (Figure 1), have been compared for their potential as dopants in LDS materials. When they are spin coated on substrates such as quartz or c-Si solar cells, and illuminated with UV light, they provide intense photoluminescence (PL) corresponding to the red emission of Eu(III) (Figure 2), or in the case of [TbL_3], to the green emission of Tb(III). The spectroscopic properties of the different compounds and films, as well as the PV properties of the doped c-Si solar cells have been studied and characteristic values are summarized in Table 2.

3.1 [Eu$(tta)_3$phen]

Photophysical characterization of [Eu$(tta)_3$phen] in solution, in the solid state and in EVA films

The UV-visible absorption spectrum of [Eu$(tta)_3$phen] has been measured in $CHCl_3$ ([Eu$(tta)_3$phen] = 1.7 $\times 10^{-5}$ M, Figure S1) and displays typical absorption bands of the 1,10-phenantroline centered at 273 nm (ε= 42900 $M^{-1}.cm^{-1}$) and of the TTA centered at 341 nm (ε= 44500 $M^{-1}.cm^{-1}$). Excitation spectra point to an efficient sensitization of the Eu(III) excited states through the TTA antennae. Excitation at 350 nm gives rise to intense Eu(III) emission, which luminescence lifetime has been measured in the solid state and is in very good agreement with literature data (τ = 0.87 ms)[39]. Emission spectra are characterized by a hypersensitive $^5D_0 \rightarrow {}^7F_2$ transition (Figure S2). Moreover, three crystal-field levels could be observed for the $^5D_0 \rightarrow {}^7F_1$transition, which indicates that the site symmetry of the Eu(III)ion is low[41]. Similar patterns were observed in the EVA polymeric films and the transmittance, PL and PLE of the [Eu$(tta)_3$phen] complex in EVA are shown in Figure 3. As expected, strong absorption is observed in the 300-400 nm region, with a maximum at 345 nm, as observed in solution and the absorption increases with the complex concentration as

seen in Fig. 3a. Under excitation at 350 nm, the modified EVA provides typical PL at 610 nm, corresponding to the emission of Eu(III). The photoluminescence quantum yield of the [Eu(tta)$_3$phen] complex in EVA has been measured by absolute methods and amounts to 60% (λ_{ex}= 360 nm). Moreover, the value is constant with excitation wavelengths ranging from 320 to 380 nm. It is in very good agreement with the quantum yield in the solid states (69%)[39], which points to a weak interaction between the complex and the EVA matrix. As a comparison, quantum yields of 73% and 72% have been reported for doped polymethylmethacrylate (PMMA) and polystyrene (PS) films, respectively[33].

Coating on c-Si solar cells and evaluation of the conversion efficiency of the LDS materials

The complex in EVA was then coated on c-Si solar cells. Figure 3c shows the EQE of a cell without coating, a similar cell with pure EVA coating and two cells with different complex concentrations. As can be seen, an increase in the UV of up to 8% absolute is observed when the cell is coated with EVA. This corresponds to purely optical effects due to the combination of optical indexes. A further increase of 10% absolute (respectively 17% absolute) is observed when the complex is mixed with EVA at a concentration of 0.3% (respectively 0.5%). A further increase of the complex concentration does not lead to further enhancement (not shown), indicating that the maximum of the effect is already obtained for a concentration of 0.5%. For all the compounds, internal quantum efficiency (IQE) was also evaluated and it shows similar trends, proving that the effects are not coming from antireflective properties (see Fig. S4). Despite the increase of EQE observed in the UV, the short circuit current and conversion efficiency of the solar cell decrease after addition of the modified EVA. This can be explained by the small loss of EQE observed in the visible part of the spectrum shown in Fig. 3c), which can originate from a parasitic absorption in the visible region observed in Fig. 3a).

3.2 [Eu(tta)$_3$(tppo)$_2$]

Photophysical characterization of [Eu(tta)$_3$(tppo)$_2$] in solution, solid state and in EVA films

In order to further identify the important parameters for our application, the [Eu(tta)$_3$(tppo)$_2$] complex, which apparently possess very similar photophysical properties in terms of excitation and emission quantum yield, has been tested. Indeed, a quantum yield of 73% has

been previously reported in the solid state with a corresponding luminescence lifetime $\tau = 0.5$ ms[40]. In our case, long-lived Eu(III) luminescence with $\tau = 0.63$ ms was observed when exciting at 350 nm and the emission spectrum also points to a low symmetry of the coordination sphere (Figure S3). The UV-visible absorption spectrum has also been measured in $CHCl_3$ $[Eu(tta)_3(tppo)_2] = 1.5 \times 10^{-5}$ M (Figure S1) and displays typical absorption bands of the triphenylphosphineoxide centered at 268 nm and 274 nm (ε= 19600 and 19800 $M^{-1}.cm^{-1}$, respectively) and of the TTA centered at 342 nm (ε= 44800 $M^{-1}.cm^{-1}$). The main difference between this complex and the previous one lies in the shape of their absorption spectra which is, in proportion, more important in the 300 – 400 nm region for the second complex. Figure 4 shows the transmittance, PL and PLE of EVA integrating this complex. A strong absorption peak around 337 nm can be observed. Here again, the absorption of the first sample (EVA + 1.3% complex) is dominated by the absorption of the TTA antennae. As a consequence, the PLE better matches the transmittance spectrum. The PL is similar to the previous compound with a peak at 614 nm originating from Eu transitions and quantum yield equal to 57 % was measured upon excitation at 365 nm on quartz substrates. It was also found to be stable in the range 320-380 nm. By increasing the doping concentration (EVA + 2.7% complex), diffraction and inner-filter effect appears which are characterized by a tail between 400 nm and 800 nm and by a non-linear decrease in transmittance in the UV region.

Coating on c-Si solar cells and evaluation of the conversion efficiency of the LDS materials

EVA was coated on c-Si solar cells with two concentrations of $[Eu(tta)_3(tppo)_2]$, 1.3 wt% and 2.7 wt%. The EQE shows an improvement of around 19% absolute thanks to the complex (2.7 wt%). Only a small improvement is observed between the two concentrations, as expected from the strong diffraction observed in the transmittance spectrum. The absolute gain of EQE in the UV is similar to the previous compound. However, as opposed to the previous case, there is no decrease of EQE in the visible spectrum. Thus the short circuit and conversion efficiency are increased by a relative 1.8% and 8% respectively after the addition of the modified EVA (Table 2).

3.3 $[EuL_3]$ and $[TbL_3]$

Photophysical characterization of $[EuL_3]$ and $[TbL_3]$ in EVA films

A recent study carried out by S. Di Pietro, D. Imbert and M. Mazzanti[26] showed that these complexes are highly luminescent in the solid state, with luminescence quantum yields of 70% and 98% for Eu(III) and Tb(III), respectively. Moreover, similar values have been obtained in polyvinyl acetate (PVA) polymeric matrixes. These complexes were finally tested with the aim to further demonstrate the influence of the absorption/excitation and emission windows of the complexes on the efficiency of the LDS materials.

Figure 5 shows the transmittance, PL and PLE of [EuL_3] and [TbL_3] in EVA. The two EVA films are highly luminescent and quantum yieds of 65% and 100% (λ_{ex} = 325 nm) have been measured for the Eu(III)-doped and Tb(III)-doped polymeric films, respectively. However, the transmittance spectrum shows that high absorption is only attained at lower wavelengths in the UV, with a maximum around 262 nm. This is not optimal for the application to solar cells, as an important part of the solar UV spectrum will not be converted. This shift towards lower wavelengths is also visible in the PLE spectra of Fig. 5b).

Coating on c-Si solar cells and evaluation of the conversion efficiency of the LDS materials

Figure 5c) shows the EQE of the two complexes in EVA. An increase of the EQE by around 15% absolute is still visible at 320 and 334 nm, which is similar to the increase observed for previous measurement with solar cells coated with [$Eu(tta)_3phen$]-doped films with similar transmission properties (EVA + 0.3 wt% complex). However, whereas an increase until 400 nm was observed in the case of [$Eu(tta)_3phen$], here, a significant decrease was measured after 345 nm, which is due to the lack of absorption of the compounds at these wavelength. Nevertheless, the short circuit current after coating with [EuL_3] increased by a relative 0.8% and the conversion efficiency increased by a relative 5.7% leading to overall better properties than the [$Eu(tta)_3phen$]-coated cells. It can be explained by the absence of decrease in efficiency in the 500-900 nm range, as observed in presence of [$Eu(tta)_3phen$]. Further increase of the EQE at 320 and 334 nm could probably be obtained with higher complex concentrations. Interestingly, the response in EQE of the Eu(III) and Tb(III) complexes is very alike, despite the difference in quantum yields measured for the two films. Similar results were also obtained for the short circuit current, with an increased by a relative 1.5%, and for the conversion efficiency, which increased by a relative 4.7%. This can be explained by the shift of the Tb(III) emission spectrum towards lower wavelengths – and therefore

lower conversion efficiency – than Eu(III). In particular a strong $^5D_4 \rightarrow {}^7F_6$ transition at 480 nm was observed in the PL spectra of the Tb complex (Fig 5b).

3.4 Evaluation of the potential energy loss due to the reemission of photons outside the cell

One possible loss in the efficiency of the modified EVA + solar cell system is the reemission of photons due to the PL out of the cell. To assess this phenomenon, reflectance measurements were carried on a solar cell coated by EVA with [Eu(tta)$_3$phen]. The emission spectra of the sample, upon varying the excitation wavelength were measured inside an integration sphere. Figure 6 shows the total reflectance measured. The shape of the curve is influenced by the SiN antireflective coating present in the cell. The second curve shows the partial reflectance due to the PL; in this case only the reflectance around 610 nm was detected while the excitation was varied from 300 to 800 nm (see Supplementary Material for mathematical treatment of the data). What can be seen in Fig. 6 is that the partial reflectance due to the PL is very small compared to the total reflectance. For example at 325 nm the total reflectance is 23% while the partial reflectance is only 3.5%. This provides evidence that the losses of photons reemitted to the air side is very small. This can be explained by the combination of optical indexes; the modified EVA plays the role of a waveguide which prevents the loss of photons. Therefore, while in some downconversion or downshifting systems additional concepts were proposed to limit the photons loss to the air side[42], in the present case such systems are not necessary.

4. Conclusion

In conclusion, four coordination complexes were dispersed in EVA and tested on c-Si solar cells. Three complexes based on Eu(III) with quantum yields of *ca.* 70% in the solid states were compared, of which the most promising system is [Eu(tta)$_3$(tppo)$_2$] and allows a gain of 19% absolute in the EQE and a relative gain of 8% in the conversion efficiency of the solar cells. In the other cases, lower gains and even losses in conversion efficiency were observed and were attributed either to an unsuitable excitation window or to parasitic absorption in the visible. Finally, a Tb(III) complex with a quantitative quantum yield was tested. Results were nevertheless very similar to the Eu(III) analogues, showing that the 30% increase in quantum yield was not enough to compensate for the loss in conversion in efficiency of the down-shifted photons in a region where the c-Si is less optimal (480 nm). This study reveals that the

complexes quantum yield is not the only important parameter in optimizing the properties of Ln(III)-based luminescent downshifting materials. Other parameters such as absorption, excitation and emission wavelengths are other critical aspects that need to be taken into account. We are currently working in that direction by developing other Eu(III)-doped polymeric matrixes with improved luminescence properties. Although some rather expensive c-Si solar cells can present a high EQE in the ultraviolet, the encapsulants such as EVA contain chemicals that are designed to absorb in the ultraviolet and prevent yellowing. Thus the present approach is still interesting for these cells, especially if higher quantum yields of the LDS layer can be obtained. Also, the work presented can be applied to CIGS solar cells where the losses from the CdS window layer in the ultraviolet can be partially recovered by photon conversion.

Acknowledgments: The authors thank S. Roques for solar cell fabrication and S. Gobron for additional experiments. This research was partially funded by the Centre National de la Recherche Scientifique exploratory project grant “CODOPER”.

[1] H. Z. Lian, Z. Y. Hou, M. M. Shang, D. L. Geng, Y. Zhang, J. Lin, Energy, 57, 270 (2013).

[2] H. J. Hovel, R. T. Hodgson, J. M. Woodall, Sol. Energ. Mat. 2, 19 (1979).

[3] T. Trupke, M. A. Green, P. Würfel, J. Appl. Phys., 92(3), 1668 (2002).

[4] B.S. Richards, Sol. Energ. Mat. Sol. C., 90(9), 1189 (2006).

[5] N. Bloembergen, Phys. Rev. Lett., 2(3), 84 (1959).

[6] F. Auzel, Cr. Acad. Sci. B, 262(15), 1016, (1966).

[7] V. Ovsyankin, P.P. Feofilov, JETP Letters, 3(12), 322 (1966).

[8] X. Huang, S. Han, W. Huang and X. Liu, Chem. Soc. Rev. 42 (2013) 173.

[9] T. Fix, G. Ferblantier, H. Rinnert, A. Slaoui, Sol. Energ. Mat. Sol. Cells 132, 191 (2015).

[10] T. Fix, J.-L. Rehspringer, H. Rinnert, A. Slaoui, Sol. Energ. Mat. Sol. Cells 133, 87 (2015).

[11] T. Fix, H. Rinnert, M.G. Blamire, A. Slaoui, and J.L. MacManus-Driscoll, Sol. Energ. Mat. Sol. Cells **102**, 71 (2012).

[12] E. Klampaftis, D. Ross, K. R. McIntosh, B. S. Richards, Sol. Energ. Mat. Sol. Cells 93, 1182 (2009).

[13] E. Klampaftis, M. Congiu, N. Robertson, and B. S. Richards, *IEEE J. Photovolt.*1 (2011) 29.

[14] T. Monzón-Hierro, J. Sanchiz, S. González-Pérez, B. González-Díaz, S. Holinski, D. Borchert, C. Hernández-Rodríguez, R. Guerrero-Lemus, Sol. Energ. Mat. Sol. Cells 136, 187 (2015).

[15] T. Fukuda, S. Kato, E. Kin, K. Okaniwa, H. Morikawa, Z. Honda, N. Kamata, Opt. Mat. 32, 22 (2009).

[16] H. Kataoka, S. Omagari, T. Nakanishi, Y. Hasegawa, Opt. Mat. 42, 411 (2015)

[17] J. Liu, K. Wang, W. Zheng, W. Huang, C.-H. Li, and X.-Z. You, Prog.Photovolt: Res. Appl. 21, 668 (2013).

[18] A. Le Donne, M. Acciarri, D. Narducci, S. Marchionna, S. Binetti, Prog. Photovolt: Res. Appl., 17, 519 (2009).

[19] A. Le Donne, M. Dilda, M. Crippa, M. Acciarri, S. Binetti, Opt. Mater., 33, 1012 (2011).

[20] S. González-Pérez, J. Sanchiz, B. González-Díaz, S. Holinski, D. Borchet, C. Hernández-Rodríguez, R. Guerrero-Lemus, Surf. Coat. Tech., 271, 106 (2015).

[21] H. Zhang, H. Song, B. Dong, L. Han, G. Pan, X. Bai, L. Fan, S. Lu, H. Zhao and F. Wang, J. Phys. Chem. C 112, 9155 (2008).

[22] A. P. Alivisatos, W. Gu and C. Larabell, Annu. Rev. Biomed. Eng. **7**, 55 (2005).

[23] X. Gao, L. Yang, J. A. Petros, F. F. Marshall, J. W. Simons and S. Nie, Curr. Opin. Biotechnol. 16, 63 (2005).

[24] M. Merchán, T. S. Ouk, P. Kubát, K. Lang, C. Coelho, V. Verney, S. Commereuc, F. Leroux, V. Sol and C. Taviot-Guého, J. Mater. Chem. B 1, 2139 (2013).

[25] J.-C. G. Bünzli, A.-S. Chauvin, num. Ch. 261, p. 169-281, Handbook on the Physics and Chemistry of Rare Earths 44 (2014).

[26] S. D. Pietro, D. Imbert and M. Mazzanti, Chem. Commun. 50, 10323 (2014) ; S. Di Pietro, N. Gautier, D. Imbert, J. Pecaut, M. Mazzanti, Dalton Trans. 45, 3429 (2016).

[27] M. Starck, P. Kadjane, E. Bois, B. Darbouret, A. Incamps, R. Ziessel and L. J. Charbonnière, Chem. – Eur. J. 17, 9164 (2011).

[28] E. Brunet, O. Juanes, R. Sedano and J.-C. Rodríguez-Ubis, Photochem. Photobiol. Sci. 1, 613 (2002).

[29] M. Latva, H. Takalo, V. M. Mukkala, C. Matachescu, J. C. Rodriguez-Ubis, J. Kantare, J. Lumin.75, 149 (1997).

[30] J.-C. G. Bünzli, S. V. Eliseeva, Chem. Sci., 4, 1939 (2013).

[31] J.-C. G. Bünzli, Coord. Chem. Rev., 293, 19 (2015).

[32] A. Badiee, R. Wildman, I. Ashcroft, Reliability of photovoltaic cells, modules, components and systems VII, Proceedings of SPIE vol. 9179 (2014).

[33] O. L. Malta, H. F. Brito, J. F. S. Menezes, F. R. Gonçalues e silva, C. de MelloDonegá, S. Alues Jr, Chem. Phys. Lett. 282, 233 (1998).

[34] J. Garcia-Torres, P. Bosch-Jimenez, E. Torralba-Calleja, M. Kennedy, H. Ahmed, J.Doran, D. Gutierrez-Tauste, L. Bautista, M. DellaPirriera, J. Photoch. Photobio. A, 275, 103 (2014).

[35] N. B. D. Lima, S. M. C.Gonçalves, S. A. Júnior, A. M. Simas, Sci. Rep. 3, 2395 (2013).

[36] O. Moudam, B. C. Rowan, M. Alamiry, P. Richardson, B. S. Richards, A. C. Jones, N. Robertson, Chem. Commun., 6, 649 (2009).

[37] P. Kadjane, L. Charbonnière, F. Camerel, P. P. Lainé, R. Ziessel, J. Fluoresc. 18, 119 (2008).

[38] K. Suzuki, A. Kobayashi, S. Kaneko, K. Takehira, T. Yoshihara, H. Ishida, Y. Shiina, S. Oishi and S. Tobita, Phys. Chem. Chem. Phys. 11, 9850 (2009).

[39] F. R. G. e Silva, J. F. S. Menezes, G. B. Rocha, S. Alves, H. F. Brito, R. L. Longo, O. L. Malta, J. Alloys. Compd., 303-304, 364 (2000).

[40] E. E. S. Teotonio, G. M. Fett, H. F. Brito, W. M. Faustino, G. de Sá, M. C. F. C. Felinto, R. H. A. Santos, J. Lumin. 128, 190 (2008).

[41] J. H. Forsberg, Coord. Chem. Rev.10, 195 (1973).

[42] J. Goffard, D. Gerard, P. Miska, A.-L.Baudrion, R. Deturche, J. Plain, Sci. Rep. 3, 2672 (2013).

Table 1: Selected data for Eu(III) complexes previously used as LDS materials in c-Si solar cells or c-Si photovoltaic (PV) modules: encapsulant, relative short-circuit enhancement($\Delta J_{SC}/J_{SC}$), relative efficiency enhancement ($\Delta\eta/\eta$) in presence of the complexes, excitation wavelength, experimental quantum yields of the corresponding complexes in solid state and in the films.

Compound	Encapsulant	$\Delta J_{SC}/J_{SC}$ (%)[a,b]	$\Delta\eta/\eta$ (%)[a,b]	λ_{ex} (nm)	Φ_{solid} (%)	Φ_{film} (%) [τ (ms)]
[Eu(dbm)$_3$phen]	PVA 10%wt[17]	-1.15[b]	-0.06[b]	380[17]	57[17]	
[Eu(tta)$_3$phen]	PVA 10%wt[17] sol-gel silica glasses in acryl resins[15]	+0.47 [b] +2 [b]	+0.43 [b]	340[17] 365[15]	69[33]	65[15] 73, PMMA [0.52][34]
[Eu(tta)$_3$bpy]	PVA 10%wt[17]	-1.15 [b]	-0.06 [b]	340[17]	66	
[Eu(tta)$_3$bpbpy]	PVA 10%wt[17]	+1.99 [b]	+1.99 [b]	340[17]	79	
[Eu(hfa)$_3$(dpepo)]	EVA[13]	<0[b]	<0 [b]	340[13] 340[35]		88 / 56[c13] 85, PMMA [0.77][36]
[Eu(hfa)$_3$(tppo)$_2$]	PMMA-St beads in EVA films[16]	+1.2[a]		300[13]		[0.71][13]
[Eu$_2$(phen)$_2$(bz)$_6$]	PMMA 2%wt[14]		+0.2 [a]			
[Eu$_2$(phen)$_2$(PFbz)$_6$]	PMMA 10%wt[20]					
[Eu(tfc)$_3$: EABP] 1:1	EVA[19]		+ 2.9[b]			
[Eu(tfc)$_3$/Eu(dbm)$_3$phen] *(2 layers)*	PVA[18]	+1.1[a]	+2.8 [a]			

[a]c-Si solar cells ; [b]c-Si PV modules ; [c]before/after lamination

Table 2: Selected photophysical properties of the [Eu(tta)$_3$phen], [Eu(tta)$_3$(tppo)$_2$], [EuL$_3$] and [TbL$_3$] complexes as well as measured relative short-circuit enhancement ($\Delta J_{SC}/J_{SC}$) and relative efficiency enhancement ($\Delta\eta/\eta$) for the complexes in EVA on c-Si solar cells. The same cells were measured before and after coating.

Compound	ε ($M^{-1}.cm^{-1}$) / λ_{abs}(nm), solvent	Φ_{solid} (%) / λ_{ex} (nm)	Φ_{EVA} (%) / λ_{ex} (nm)	$\Delta J_{SC}/J_{SC}$	$\Delta\eta/\eta$
[Eu(tta)$_3$phen]	42900 / 273 44500 / 341, $CHCl_3$	69 / 350[39]	60 / 325	-6.9%	-2.4%
[Eu(tta)$_3$(tppo)$_2$]	19600 / 268 44800 / 342, $CHCl_3$	73[40]	57 / 365	+1.8%	+8%
[EuL$_3$]	106000 / 260 23400 / 315, CH_3OH	70 / 325[26]	65 / 325	+0.8%	+5.7%
[TbL$_3$]	106000 / 260 23500 / 315, CH_3OH	98 / 325[26]	100 / 325	+1.5%	+4.7%

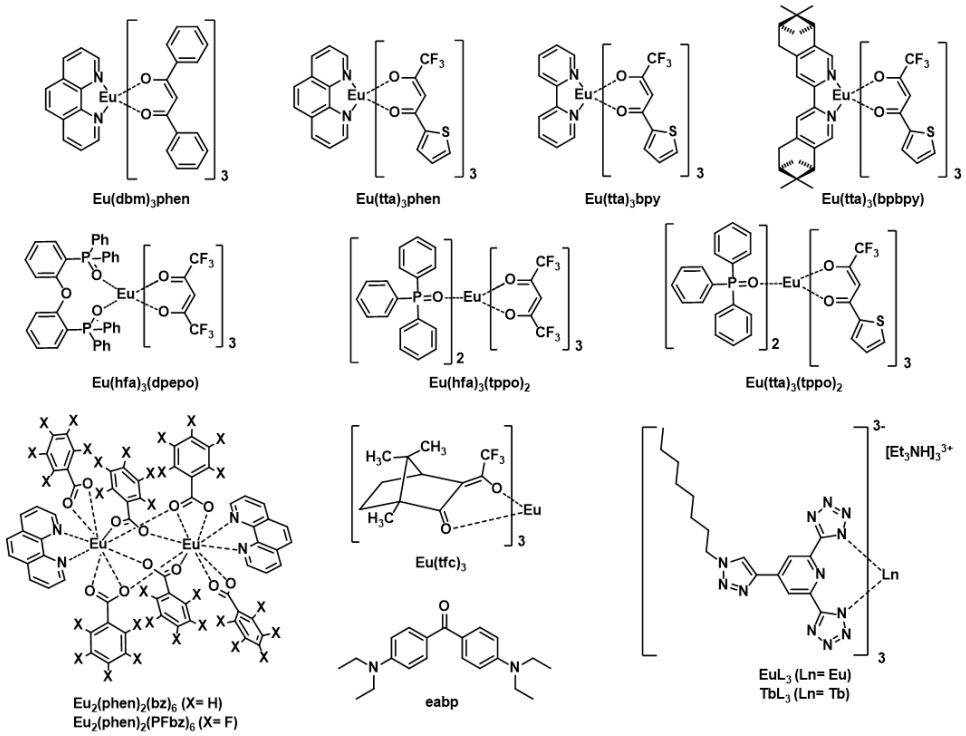

Figure 1: Structures of the coordination complexes discussed in this work.

a) b)

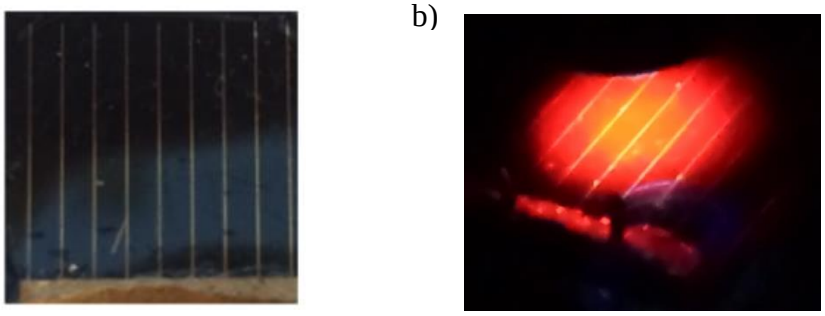

Figure 2: c-Si cell fabricated and coated with EVA including [Eu(tta)$_3$phen] a) top-view b) illuminated at a wavelength of 350 nm.

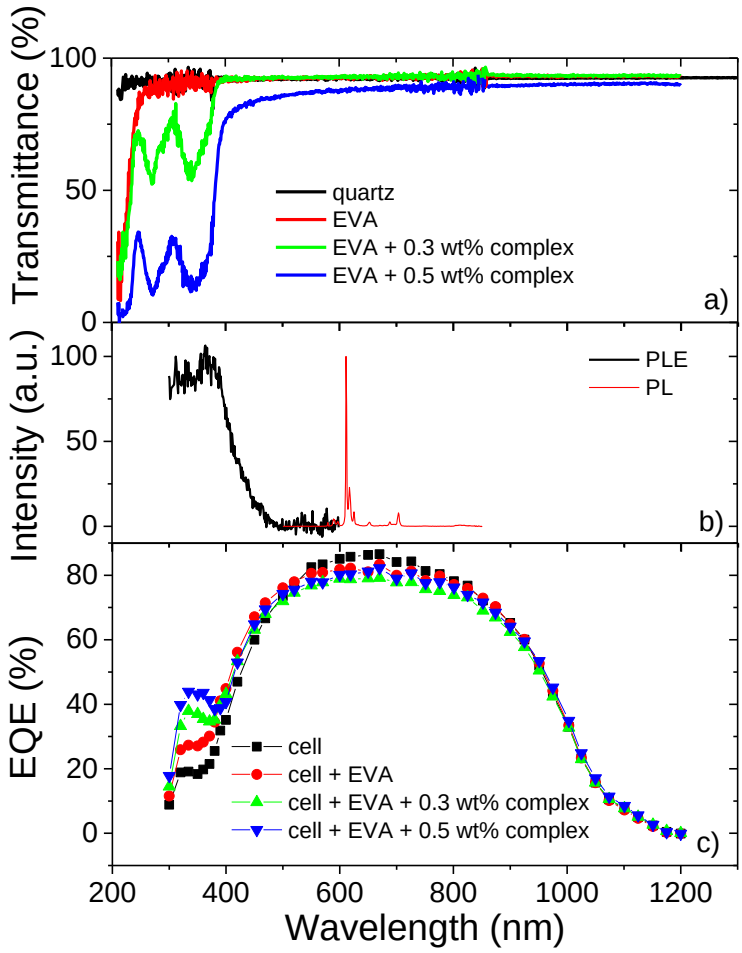

Figure 3: a) transmittance spectra of the quartz substrate, EVA-coated quartz, and EVA with two different concentrations of [Eu(tta)$_3$phen] complex. b) PL (excitation at 350 nm) and PLE (detection at 610 nm) spectra of EVA with the [Eu(tta)$_3$phen] complex on quartz substrate. c) EQE of a c-Si solar cell, a cell coated with EVA, and two cells with different concentrations of [Eu(tta)$_3$phen] complex in EVA.

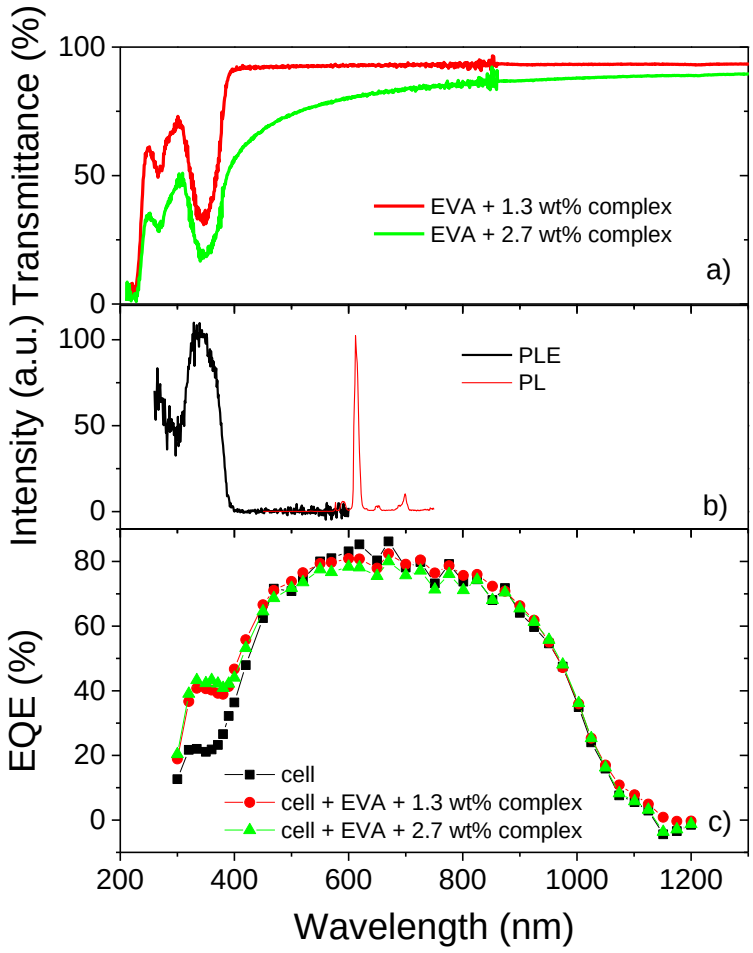

Figure 4: a) transmittance spectra of EVA with two different concentrations of $[Eu(tta)_3(tppo)_2]$ complex. b) PL (excitation at 360 nm) and PLE (detection at 610 nm) spectra of EVA with the $[Eu(tta)_3(tppo)_2]$ complex on quartz substrate. c) EQE of a c-Si solar cell and two cells with different concentrations of $[Eu(tta)_3(tppo)_2]$ complex in EVA.

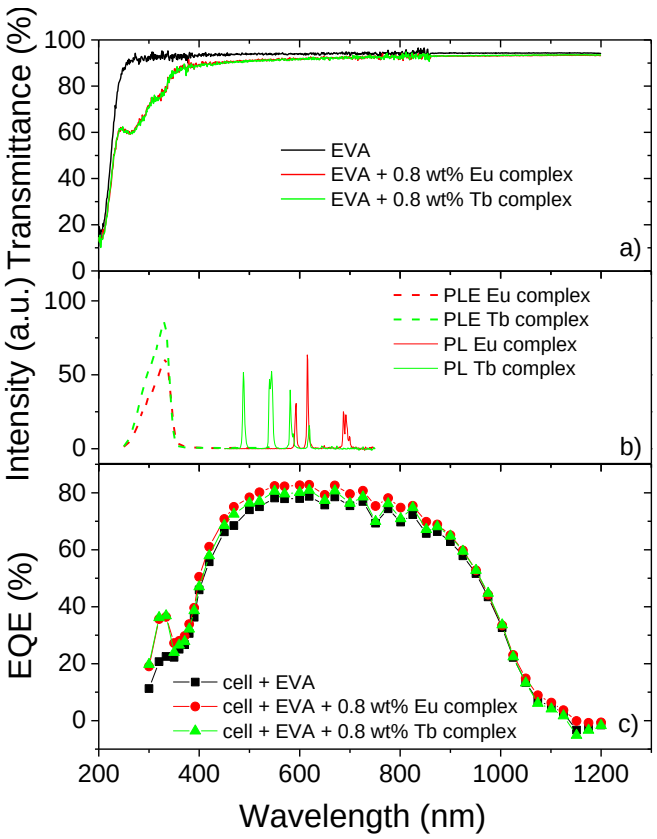

Figure 5: a) Transmittance spectra b) PL and PLE spectra of [EuL_3] and [TbL_3] complex in EVA on quartz substrates c) EQE of a c-Si solar cell and cells with [EuL_3] and [TbL_3] complexes in EVA.

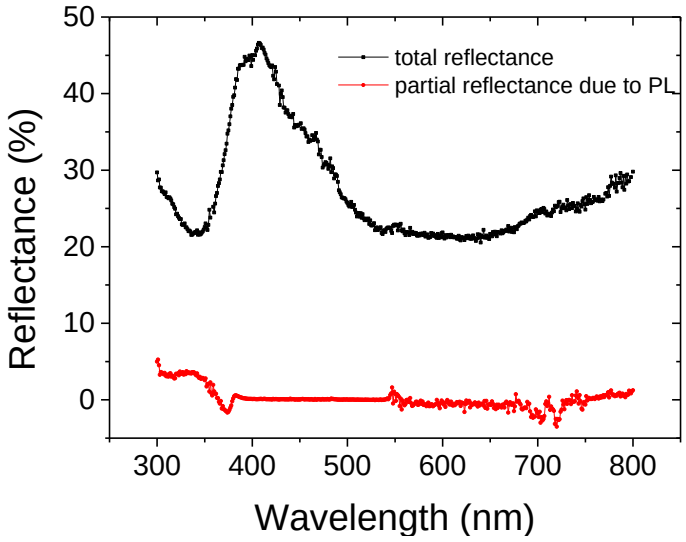

Figure 6: Total reflectance and partial reflectance due to the PL of a c-Si solar cell coated with [Eu(tta)$_3$phen] in EVA.